ELSEVIER

Journal of Physics and Chemistry of Solids 64 (2003) 247–252

JOURNAL OF PHYSICS AND CHEMISTRY OF SOLIDS

www.elsevier.com/locate/jpcs

Temperature dependence of the luminescence of nanocrystalline CdS/Mn^{2+}

Ageeth A. Bol*, Rick van Beek, Joke Ferwerda, Andries Meijerink

Physics and Chemistry of Condensed Matter, Debye Institute, Utrecht University, P.O. Box 80 000, 3508 TA Utrecht, The Netherlands

Received 29 October 2001; received in revised form 13 May 2002; accepted 14 May 2002

Abstract

The temperature dependence of the luminescence properties of nanocrystalline CdS/Mn^{2+} particles is investigated. In addition to an orange Mn^{2+} emission around 585 nm a red defect related emission around 700 nm is observed. The temperature quenching of both emissions is similar ($T_q \approx 100$ K). For the defect emission the reduction in the lifetime follows the temperature dependence of the intensity. For the Mn^{2+} emission however, the intensity decreases more rapidly than the lifetime with increasing temperature. To explain these observations a model is proposed in which the Mn^{2+} ions are excited via an intermediate state involving shallowly trapped ($\approx$40 meV) charge carriers.

Keywords: A. Nanostructures; A. Semiconductors; D. Luminescence

1. Introduction

Nowadays, it is well known that the electronic properties of nanocrystalline semiconductors change with decreasing particle size due to quantum confinement effects [1–5]. If the radius of the semiconductor particles becomes smaller than the Bohr radius of the exciton the band gap of the semiconductor increases and the edges of the bands split into discrete energy levels. In the last two decades these quantum confinement effects have stimulated great interest in both basic and applied research.

The luminescence of Mn^{2+} ions in quantum sized nanocrystalline sulphides like ZnS became a popular field of research after it was reported that nanocrystalline ZnS/Mn^{2+} yields high luminescence quantum yields and lifetime shortening at the same time due to quantum confinement effects [6]. Even though it was shown later that the lifetime shortening of the Mn^{2+} emission in nanocrystalline ZnS/Mn^{2+} was due to a misinterpretation [7,8], the luminescence of various luminescent ions in different II–VI semiconductors has been studied extensively. One of the systems that have been investigated is nanocrystalline CdS/Mn^{2+} [9–13]. In nanocrystalline CdS/Mn^{2+} both an orange (585 nm) emission and a red emission (~700 nm) have been observed. The orange emission has been assigned to the $^4T_1 \rightarrow {}^6A_1$ transition on Mn^{2+} and the red emission to defects in CdS. The lifetime of the Mn^{2+} related emission is in the ms range [9–11], in agreement with the long ms lifetime observed for Mn^{2+} in nanocrystalline ZnS/Mn^{2+} [7,8].

Some groups have proposed models on the mechanism of luminescence for nanocrystalline CdS/Mn^{2+}. Levy et al. [12] suggested that after excitation of the nanocrystalline CdS host, energy will be transferred from the conduction band of the CdS host to the $^4T_1$ level of the Mn^{2+} impurity or to defect states, resulting in emissions around 590 and 700 nm, respectively. Liu et al. [13] proposed that after host lattice excitation the excited charge carriers are trapped rapidly by localised surface states, followed by energy transfer from these surface states to the $^4T_1$ level of the Mn^{2+} impurity, from which radiative decay to the $^6A_1$ ground state of the Mn^{2+} ion occurs.

To investigate the mechanism of luminescence for nanocrystalline CdS/Mn^{2+} in more detail this report deals with temperature dependent luminescence and lifetime measurements on nanocrystalline CdS/Mn^{2+} and $Cd_xZn_{1-x}S/Mn^{2+}$.

* Corresponding author. Present address: Philips Research, Prof. Holstlaan 4 (WA11), 5656 AA Eindhoven, The Netherlands. Tel.: +31-40-2742271; fax: +31-30-2744282.

E-mail address: ageeth.bol@philips.com (A.A. Bol).

0022-3697/03/$ - see front matter © 2002 Elsevier Science Ltd. All rights reserved.
PII: S0022-3697(02)00286-X

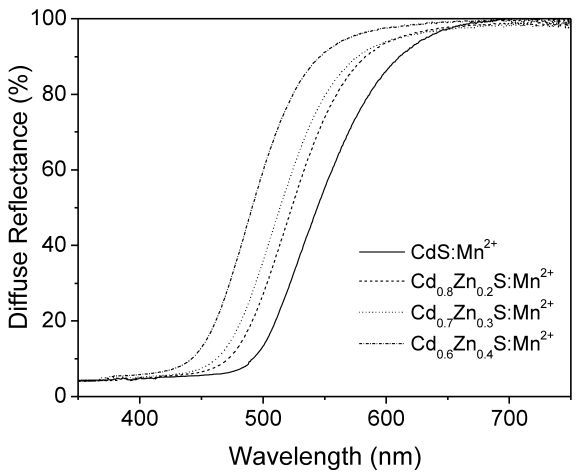

Fig. 1. UV–VIS reflection spectra of nanocrystalline $Cd_xZn_{1-x}S/Mn^{2+}$.

2. Experimental

The synthesis route followed to make nanocrystalline CdS/Mn^{2+} resembles standard methods for synthesis of nanocrystalline II–VI semiconductors. The method used for the synthesis of nanocrystalline CdS/Mn^{2+} coated with sodiumpolyphosphate (PP) is very similar to the one we used for the synthesis of nanocrystalline ZnS/Mn^{2+} and ZnS/Pb^{2+} [7,14]. Ten millilitre, 1 M $Cd(ClO_4)_2{\cdot}6H_2O$ and 10 or 25 ml 0.1 M $Mn(ClO_4)_2{\cdot}6H_2O$ were added to an aqueous solution of 10.2 g $Na(PO_3)_n$ (Aldrich, 96%, $n \sim 10$). The total volume after the addition was 90 ml. After about 10 min of stirring, 10 ml of a 1 M $Na_2S{\cdot}9H_2O$ solution was injected into the solution. Immediately after the injection of the Na_2S solution a turbid orange fluid was obtained. Then the particles were centrifuged, rinsed with distilled water and ethanol, and dried in vacuum. Samples of $Cd_xZn_{1-x}S/Mn^{2+}$ were prepared in the same way as ascribed earlier. The only difference is that $10x$ ml of 1 M $Cd(ClO_4)_2{\cdot}6H_2O$ and $10(1-x)$ ml of 1 M $Zn(ClO_4)_2{\cdot}6H_2O$ was used instead of 10 ml of 1 M $Cd(ClO_4)_2{\cdot}6H_2O$.

X-ray powder diffraction patterns of the samples were obtained with a Philips PW 1729 X-ray generator with Cu Kα radiation ($\lambda = 1.542$ Å). From the line width the particle diameter was calculated using the Scherrer formula [15]. Diffuse reflection spectra were measured using a double beam Perkin–Elmer Lambda 16 UV/VIS spectrophotometer.

Emission and excitation spectra were recorded on a SPEX Fluorolog spectrophotometer model F2002, equipped with two double grating 0.22 m monochromators (SPEX 1680) and a 450 W Xenon lamp as excitation source. The emission was detected with a cooled Hamamatsu R928 photomultiplier. In some cases an ARC Spectro Pro®-300i monochromator and a Princeton Instruments CCD camera were used to measure emission spectra.

For lifetime measurements at an excitation wavelength of 355 nm the third harmonic of a Quanta Ray Nd/YAG laser was used. The emission was detected by an ARC Spectro Pro®-300i monochromator and a RCA c31034 photomultiplier tube or by a Spex 1269 1.26 m monochromator and a Hamamatsu R928P photomultiplier (thermoelectrically cooled to −30 °C).

Decay curves were measured with a Tektronix 2440 digital oscilloscope. Temperature dependent measurements were performed using an Oxford Instruments liquid helium flow cryostat for temperatures ranging from 4.2 K to room temperature.

3. Results and discussion

UV–Vis reflection spectroscopy and X-ray diffraction have been used to study the absorption characteristics and size of the CdS/Mn^{2+} and $Cd_xZn_{1-x}S/Mn^{2+}$ nanoparticles. Fig. 1 shows diffuse reflection spectra of nanocrystalline CdS/Mn^{2+} and $Cd_xZn_{1-x}S/Mn^{2+}$ ($x = 1$, 0.8, 0.7 and 0.6). The onset of absorption (the point were the diffuse reflection becomes smaller than 100%) is a measure for the size of the band gap of the semiconductor. For nanocrystalline CdS/Mn^{2+} a broad absorption band with an absorption onset at 650 nm is observed. The tail in the absorption spectrum extends to longer wavelengths than for bulk CdS. This is probably due to sulphur or MnS contamination, which absorb in this region. The spectral position of the absorption maximum explains the orange colour of the sample. The position of the absorption band is very close to that of bulk CdS. This is in agreement with the fact that the radius of the CdS particles (~2.5 nm) is similar to the exciton Bohr radius (2.5 nm) in CdS. In this size regime only weak quantum size effects are present.

The band gap of bulk CdS is smaller (2.5 eV) than the band gap of bulk ZnS (3.7 eV) [16]. By admixing small amounts of Zn into the CdS lattice the band gap of the system increases. This is also illustrated in Fig. 1. By admixing 0–40% of Zn^{2+} into the CdS lattice the band gap increases and the onset of the absorption band shifts to higher energies.

The XRD patterns of nanocrystalline CdS/Mn^{2+} show broad bands due to the finite size of the nanocrystals. Due to the line broadening it is difficult to deduce whether the nanocrystals have the wurtzite or the zincblende structure of CdS. Both modifications have been reported for nanocrystalline CdS, although the zincblende structure is the most common modification for nanoparticles prepared in solution. From the line broadening of the XRD pattern the average particle diameter was calculated using Scherrer's formula [15]. The average particle diameter was around 4.5 nm for all samples.

In Fig. 2 a typical example of an emission and excitation spectrum of nanocrystalline CdS/Mn^{2+} measured at 4 K is

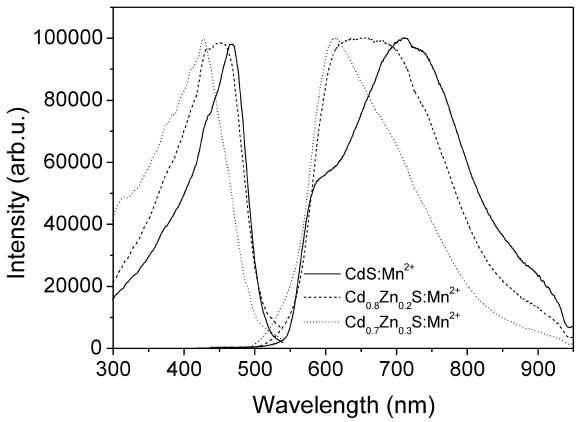

Fig. 2. Excitation and emission spectra of nanocrystalline $Cd_xZn_{1-x}S/Mn^{2+}$ ($x = 0$, 0.8 and 0.7, respectively) measured at 4 K. The excitation spectra were measured for an emission wavelength of 585, 595 and 595 nm, respectively. The emission spectra were recorded for 450, 450 and 425 nm excitation, respectively.

shown. The emission spectrum shows a broad band extending from 500 to 850 nm. The shoulder at about 585 nm corresponds to the $^4T_1 \rightarrow {}^6A_1$ transition of the Mn^{2+} impurity [17]. The emission around 700 nm is also observable for undoped nanocrystalline CdS and is assigned to a defect related CdS emission [18]. The excitation spectrum has its maximum around 450 nm and has shifted to the blue compared to the excitation spectrum of bulk CdS due to quantum confinement effects.

Fig. 2 also shows the excitation and emission spectra of several $Cd_xZn_{1-x}S/Mn^{2+}$ (10% Mn^{2+} precursor concentration) samples measured at 4 K. With increasing Zn^{2+} amount used in the synthesis the excitation spectrum shifts to the blue due to the increase of the band gap of the material, as was also illustrated in the diffuse reflection spectra (Fig. 1). The CdS related defect emission shifts to the blue accordingly, while the spectral position of the Mn^{2+} emission does not change, as far as can be deduced. The shift of the defect related emission in (nanocrystalline) semiconductors as the band gap changes indicates that a delocalised charge carrier is involved [19]. As the band gap changes, the energy of the delocalised (shallowly trapped) charge carrier follows the energy shift of the conduction or valence band and influences the wavelength of the emission band.

In Fig. 3 the temperature dependence of the emission of nanocrystalline CdS/Mn^{2+} (25% precursor concentration) is shown. With increasing temperature both the Mn^{2+} emission and the CdS related emission quench rapidly. Above 250 K the emission has totally quenched. The quenching temperature of the emission (T_q) is defined as the temperature at which the emission reaches half of its maximum intensity. Both the Mn^{2+} emission and the CdS related emission have a quenching temperature of 100 K.

By admixing Zn^{2+} into the host lattice the temperature

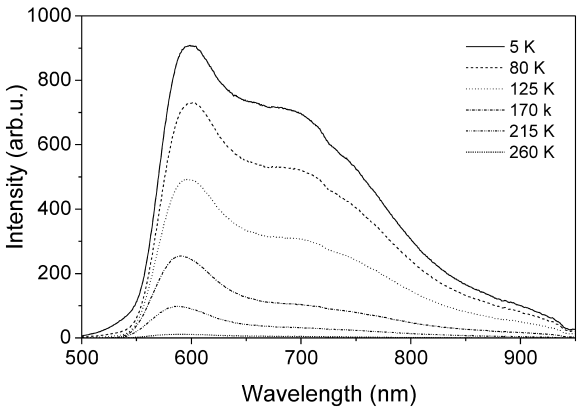

Fig. 3. Temperature dependence of the emission spectrum of nanocrystalline CdS/Mn^{2+} (25% Mn^{2+} precursor concentration) measured for 455 nm excitation.

quenching of the emissions does not change: for all samples both emissions quench at the same rate (Fig. 4). For all $Cd_xZn_{1-x}S/Mn^{2+}$ samples quenching temperatures of around 100 K were found for both emissions. Similar temperature dependence has been reported for the Mn^{2+} emission of nanocrystalline CdS/Mn^{2+} in Ref. [20]. A model that can explain the similar temperature dependence of the Mn^{2+} and the CdS related emission is shown in Fig. 5. After excitation in the CdS host (1) the excited charge carriers are trapped in shallow trap states. In Fig. 5 the situation is shown assuming that electrons are trapped in states just below the conduction band (2). A similar picture can be drawn for holes (based on the present results it is not possible to distinguish between the two possibilities). This trapping of charge carriers is followed by either energy transfer to the $^4T_1$ excited state of a Mn^{2+} ion (3), or

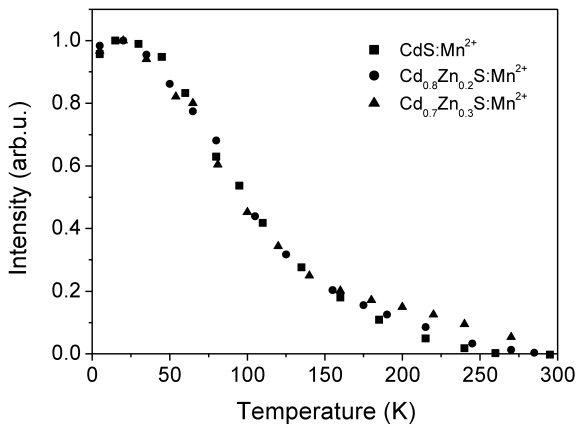

Fig. 4. Luminescence intensity of the Mn^{2+} emission (600 nm) as a function of temperature for nanocrystalline CdS/Mn^{2+}, $Cd_{0.8}Zn_{0.2}S/Mn^{2+}$ and $Cd_{0.7}Zn_{0.3}S/Mn^{2+}$ (10% Mn^{2+} precursor concentration). The samples were excited 470, 450 and 425 nm, respectively. The curves are normalised at maximum luminescence intensity.

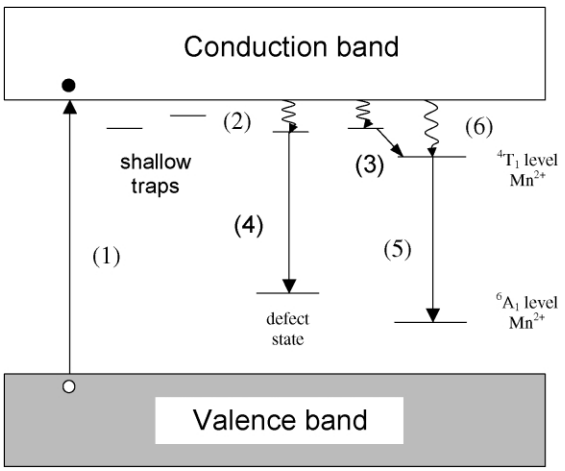

Fig. 5. Schematic representation of the proposed mechanism of the luminescence of nanocrystalline CdS/Mn^{2+}.

radiative recombination with a deeply trapped hole at a defect state (4) (CdS related emission at around 700 nm). Step (3) is followed by radiative decay from the $^4T_1$ excited state to the $^6A_1$ ground state of the Mn^{2+} ion (5) giving the orange Mn^{2+} luminescence. With increasing temperature the shallow traps just below the conduction band are thermally emptied. This results in a decrease of both the defect related CdS emission and the Mn^{2+} emission in a similar way. If the $^4T_1$ excited state of the Mn^{2+} ion was directly filled from the conduction band (6) the quenching temperature of the CdS emission and the Mn^{2+} related emission would be expected to be different.

By admixing Zn^{2+} into the host lattice the band gap of the material increases. This does not influence the quenching temperature of both emissions. From this it is concluded that the shallow traps shift with the conduction band to higher energies as is usually observed for shallowly trapped charge carriers [19]. Furthermore, this is in agreement with the interpretation that the Mn^{2+} ion is excited via the shallow trap states and not directly from the conduction band. If the latter was true the quenching temperature of the Mn^{2+} emission would be influenced by the size of the band gap, since the Mn^{2+} energy levels are not expected to shift in energy by changes in band gap due to admixing small amounts of Zn in the CdS host lattice.

Using Arrhenius equation the activation energy needed to detrap the charge carriers from the shallow trap states to the conduction band was calculated from the temperature dependence of the emission intensity. An activation energy of 41 meV (±5 meV) was found for both emissions.

To investigate the luminescence mechanism of nanocrystalline CdS/Mn^{2+} in more detail the lifetimes of both the Mn^{2+} emission and the CdS related emission were measured. In Fig. 6 typical decay curves measured for the Mn^{2+} emission and the CdS related emission are shown. The decay curves of both emissions were fitted with a one-exponential decay function, which gave satisfactory results

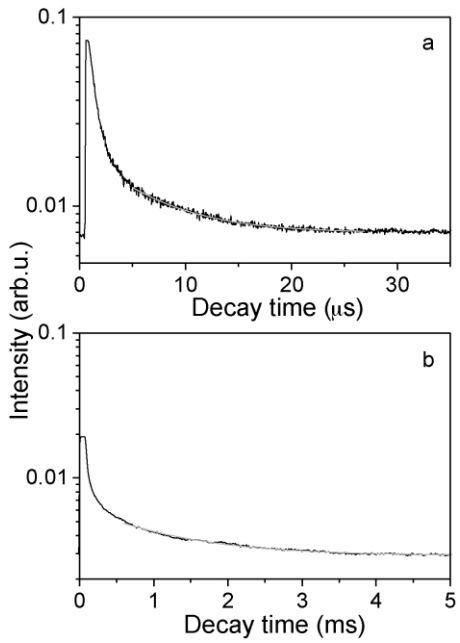

Fig. 6. Typical decay curves measured for nanocrystalline CdS/Mn^{2+} (10% Mn^{2+} precursor concentration). The sample was excited at 355 nm and the decay curves were measured at an emission wavelength of (a) 710 and (b) 605 at 65 K.

for the longer time regime. A non-exponential initial decay component is also present.

The temperature dependence of the lifetimes of both emissions of nanocrystalline CdS/Mn^{2+} are shown in Fig. 7, together with the temperature dependence of the intensity of the emissions. The lifetime of the CdS related emission is about 6 μs at 4 K. At higher temperatures the decay time decreases to about 0.3 μs at 150 K. As can be seen in Fig. 7(a) the rate of the decrease of the lifetime of the CdS emission follows the decrease of the intensity of this emission. This is consistent with the previously proposed model in which it was assumed that the CdS related emission originates from shallow trap states. At elevated temperatures these trap states are thermally emptied, which causes a decrease of both the intensity and the lifetime of the emission at the same rate. Above 100 K the life time decreases faster with increasing temperature than the emission intensity. This indicates that in this temperature regime also the radiative decay rate is increased. This causes a drop in lifetime, without affecting the emission intensity.

The lifetime of the Mn^{2+} emission is approximately 1 ms at 4 K and comparable to the lifetime reported for the Mn^{2+} emission in bulk CdS/Mn^{2+} (0.65 ms [21]). The lifetime is a factor of 2 smaller than the lifetime of the Mn^{2+} emission in nanocrystalline ZnS/Mn^{2+} [7]. This can possibly be explained by the fact that the Cd^{2+} ion is heavier than the Zn^{2+} ion (average relative atomic masses 112.4 and 65.4, respectively [22]). An interaction between the heavy neighbouring Cd^{2+} ions (with a relative high spin-orbit

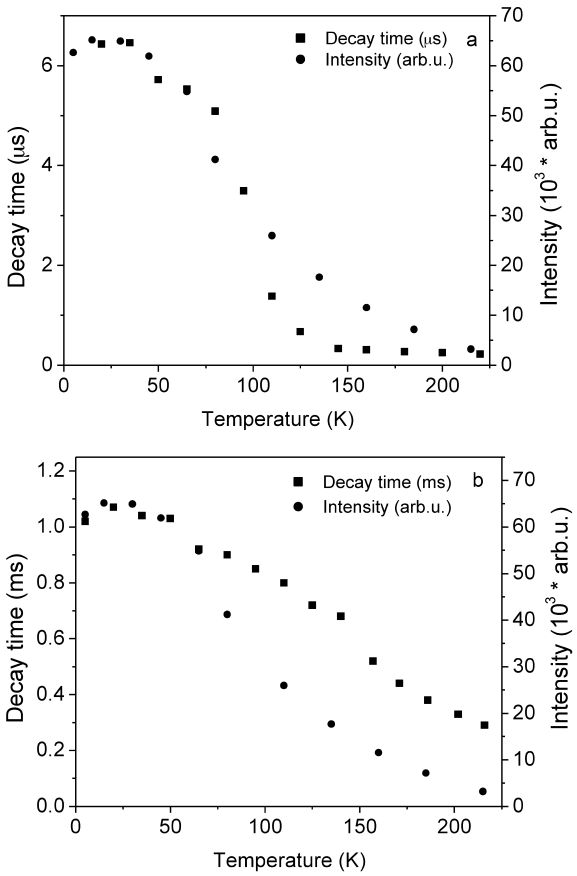

Fig. 7. Lifetime and intensity of (a) the CdS related emission (λ_{em} = 710 nm) and (b) the Mn^{2+} related emission (λ_{em} = 605 nm) of nanocrystalline CdS/Mn^{2+} (10% Mn^{2+} precursor concentration) plotted as a function of temperature. For the decay time measurements the sample was excited with 355 nm radiation, while for the luminescence measurements 470 nm radiation was used.

coupling) and the Mn^{2+} luminescent centre can cause an increase of the spin-orbit coupling of the Mn^{2+} ion, which leads to relaxation of the spin selection rule. This causes a lower luminescent lifetime of the Mn^{2+} in CdS. This effect is analogous to the so-called external heavy atom effect [23] observed for organic molecules. By interaction between a heavy atom with a strong spin-orbit coupling (such as I^- [24], Tl^+ [25] or rare earth ions [26]) the spin selection rule is partially lifted.

As can be seen in Fig. 7(b) the decay time of the Mn^{2+} emission decreases slower with increasing temperature than the emission intensity. This provides further evidence that the excited state of the Mn^{2+} ion ($^4T_1$) is fed by the shallow delocalised traps from which the CdS related emission originates. The decrease of the intensity of the Mn^{2+} emission is then caused by the thermally activated emptying of the shallow traps. This process does not influence the lifetime of the Mn^{2+} emission. The decrease of the lifetime

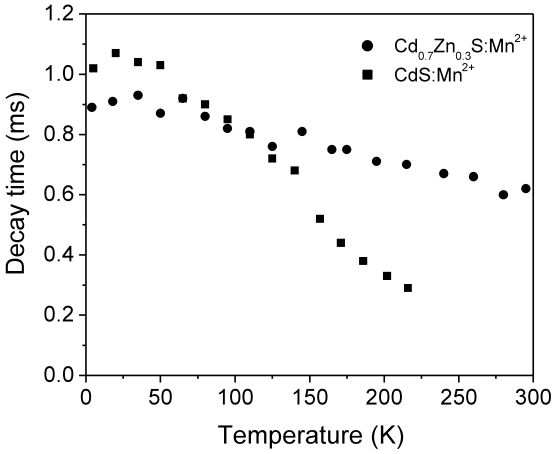

Fig. 8. Decay times of the Mn^{2+} emission (λ_{em} = 600 nm) of nanocrystalline CdS/Mn^{2+} and $Cd_{0.7}Zn_{0.3}S/Mn^{2+}$ plotted as a function of temperature. The samples were excited at 355 nm.

of the Mn^{2+} emission with increasing temperature is caused by an intrinsic quenching at the Mn^{2+} ion. Therefore the decrease of the luminescence intensity does not follow the reduction of the lifetime of the emission with temperature.

In Fig. 8 the lifetime of the Mn^{2+} emission of both nanocrystalline CdS/Mn^{2+} and nanocrystalline $Cd_{0.7}Zn_{0.3}S/Mn^{2+}$ is plotted as a function of temperature. The lifetime of the Mn^{2+} emission in nanocrystalline $Cd_{0.7}Zn_{0.3}S/Mn^{2+}$ measured at 4 K is about the same as for CdS/Mn^{2+} (~1 ms). With increasing temperature the lifetime decreases. However, as it is clear from Fig. 8, the quenching rate of the lifetime of the Mn^{2+} emission is lower in nanocrystalline $Cd_{0.7}Zn_{0.3}S/Mn^{2+}$ than in nanocrystalline CdS/Mn^{2+}, indicating that the temperature induced (intrinsic) quenching of the Mn^{2+} emission does not occur in $Cd_{0.7}Zn_{0.3}S/Mn^{2+}$ below room temperature. This may be related to the wider band gap in $Cd_{0.7}Zn_{0.3}S/Mn^{2+}$ or the influence of smaller Zn^{2+} ions. Further research is required to resolve this issue.

4. Conclusion

Temperature dependent luminescence and luminescence lifetime measurements are reported for nanocrystalline CdS/Mn^{2+}. Based on the results a model is proposed in which shallow traps are involved in the energy transfer process from the exciton to Mn^{2+}.

References

[1] R. Rosetti, R. Hull, J.M. Gibson, L.E. Brus, J. Chem. Phys. 82 (1985) 552.
[2] L. Brus, J. Phys. Chem. 90 (1986) 2555.
[3] A. Henglein, Chem. Rev. 89 (1989) 1861.

[4] Y. Wang, N. Herron, J. Phys. Chem. 95 (1991) 525.
[5] A.P. Alivistatos, J. Phys. Chem. 100 (1996) 13226.
[6] R.N. Bhargava, D. Gallagher, Phys. Rev. Lett. 72 (1994) 416.
[7] A.A. Bol, A. Meijerink, Phys. Rev. B 58 (1998) R15997.
[8] N. Murase, R. Jagannathan, Y. Kanematsu, M. Watanabe, A. Kurita, K. Hirata, T. Yazawa, T. Kushida, J. Phys. Chem. B 103 (1999) 754.
[9] M.A. Chamarro, V. Voliotis, R. Grousson, P. Lavallard, T. Gacoin, G. Counio, J.P. Boilot, R. Cases, J. Cryst. Growth 159 (1996) 853.
[10] G. Counio, T. Gacoin, J.P. Boilot, J. Phys. Chem. B 102 (1998) 5257.
[11] M.V. Artemyev, L.I. Gurinovich, A.P. Stupak, S.V. Gaponenko, Phys. Stat. Sol. (b) 224 (2001) 191.
[12] L. Levy, D. Ingert, N. Feltin, M.-P. Pileni, Adv. Mater. 10 (1998) 53.
[13] S. Liu, F. Liu, H. Guo, Z. Zhang, Z. Wang, Solid State Commun. 115 (2000) 615.
[14] A.A. Bol, A. Meijerink, Phys. Stat. Solidi. B 224 (2001) 173.
[15] B.D. Cullity, Elements of X-ray Diffraction, Addison-Wesley, Massachusetts, 1978, p. 102.
[16] S. Shionoya, in: W.M. Yen, S. Shionoya (Eds.), Phosphor Handbook, CRC Press, Boca Raton, 1999, Chapter 3.
[17] D.C. Curie, R. Acad. Sci. 258 (1964) 3269.
[18] F. Henneberger, J. Puls, C. Spiegelburg, A. Scuelzgen, H. Rossman, V. Jungnickel, A.L. Ekimov, Semicond. Sci. Technol. 6 (1991) A41.
[19] A. Van Dijken, Optical Properties and Quantum Confinement of Nanocrystalline II–VI Semiconductor Particles, Chapter 3, Thesis, Utrecht University, 1999.
[20] L. Levy, D. Ingert, N. Feltin, M.P. Pileni, J. Cryst. Growth 184–185 (1998) 377.
[21] C. Ehrlich, W. Busse, H.-E. Gumlich, D. Tschierse, J. Cryst. Growth 72 (1985) 371.
[22] D.R. Lide (Eds.), Handbook of Chemistry and Physics, 74th ed., CRC Press, Boca Raton, 1993.
[23] G.G. Guilbalt (Eds.), Fluorescence: Theory, Instrumentation and Practice, Marcel Dekker, New York, 1967, p. 88.
[24] M. Braun, W. Tuffentsammer, H. Wachtel, H.C. Wolf, Chem. Phys. Lett. 307 (1999) 373.
[25] S.I. Klink, L. Grave, D.N. Reinhoudt, F.C.J.M. Van Veggel, M.H.V. Werts, F.A.J. Geurts, J.W. Hofstraat, J. Phys. Chem. A 104 (2000) 5457.
[26] F. Schael, H.-G. Loehmannsroeben, Chem. Phys. 206 (1996) 193.